

## CELL BIOLOGY

## Dissecting the biology of mTORC1 beyond rapamycin

Guang Yang<sup>1\*†</sup>, Deanne Francis<sup>1†‡</sup>, James R. Krycer<sup>1§</sup>, Mark Larance<sup>1</sup>, Ziyang Zhang<sup>2</sup>, Chris J. Novotny<sup>2||</sup>, Alexis Diaz-Vegas<sup>1</sup>, Kevan M. Shokat<sup>2</sup>, David E. James<sup>1,3\*</sup>

Rapamycin extends maximal life span and increases resistance to starvation in many organisms. The beneficial effects of rapamycin are thought to be mediated by its inhibitory effects on the mechanistic target of rapamycin complex 1 (mTORC1), although it only partially inhibits the kinase activity of mTORC1. Other mTOR kinase inhibitors have been developed, such as Torin-1, but these readily cross-react with mTORC2. Here, we report the distinct characteristics of a third-generation mTOR inhibitor called RapaLink1. We found that low doses of RapaLink1 inhibited the phosphorylation of all mTORC1 substrates tested, including those whose phosphorylation is sensitive or resistant to inhibition by rapamycin, without affecting mTORC2 activity even after prolonged treatment. Compared with rapamycin, RapaLink1 showed better efficacy for inhibiting mTORC1 and potentially blocked cell proliferation and induced autophagy. Moreover, using RapaLink1, we demonstrated that mTORC1 and mTORC2 exerted differential effects on cell glycolysis and glucose uptake. Last, we found that RapaLink1 and rapamycin had opposing effects on starvation resistance in *Drosophila*. Consistent with the effects of RapaLink1, genetic blockade of mTORC1 activity made flies more sensitive to starvation, reflecting the complexity of the mTORC1 network that extends beyond effects that can be inhibited by rapamycin. These findings extend our understanding of mTOR biology and provide insights into some of the beneficial effects of rapamycin.

## INTRODUCTION

The mechanistic (formerly known as “mammalian”) target of rapamycin (mTOR) is a critical regulator of many major cellular functions, including cell growth, proliferation, metabolism, and survival. Dysregulation of the mTOR pathway has been implicated in many human diseases, such as diabetes, epilepsy, neurodegeneration, and cancer. mTOR serves as a catalytic subunit of two functionally distinct multiprotein complexes termed mTOR complex 1 (mTORC1) and 2 (mTORC2). These complexes perform different functions in cells. mTORC1 integrates extra- and intracellular signal inputs (amino acids, growth factors, stress, and energy status) to control key biological processes that are required for cell growth and proliferation, whereas mTORC2 mainly participates in cell metabolism and survival by activating Akt, protein kinase C  $\alpha$  (PKC $\alpha$ ), and serum/glucocorticoid regulated kinase 1 (SGK1) (1–3).

There has been great interest in establishing the unique biological functions of these different mTOR complexes. One approach has involved generation of cell lines or animal models in which specific components of either the mTORC1 or mTORC2 have been genetically deleted, usually either Raptor or Rictor/SIN1, the specific subunits of the mTORC1 and mTORC2, respectively (4–7). A major limitation of these approaches is that the chronic absence of proteins with essential biological functions can lead to adaptive responses that

may or may not have physiological relevance. For instance, in mouse embryonic fibroblasts (MEFs) lacking SIN1 (4), there is loss of FOXO1/3a phosphorylation, but other Akt substrates, tuberous sclerosis complex 2 (TSC2) and glycogen synthase kinase-3 (GSK3), are unaffected, although Ser<sup>474</sup> phosphorylation of Akt is abolished. However, acute prevention of Ser<sup>474</sup> phosphorylation using a chemical genetics approach influences Akt2 activity toward several substrates, including both FOXO1/3a and TSC2 (8), indicating the existence of a compensatory mechanism in chronic knockout experiments.

To circumvent these issues, researchers have devised mTOR-specific small-molecule inhibitors that can be added acutely to cells or animals followed by dynamic monitoring of biological consequences. In the case of mTORC1, the drug rapamycin has been invaluable. The discovery of mTOR arose from characterization of this natural compound, and only mTORC1 is acutely sensitive to inhibition by rapamycin, leading to rapamycin’s use as an mTORC1 inhibitor in both fundamental and clinical research for almost 30 years (1). Rapamycin forms a complex with the 12-kDa FK506-binding protein, FRBP12, which binds to a domain adjacent to the active site of the kinase mTOR and reduces access to the active site cleft (9). Although rapamycin has been invaluable for studying mTORC1 biology, it inhibits only some of the phosphorylation events mediated by mTORC1. Thus, given that much of our knowledge about mTORC1-specific functions stems from the use of rapamycin, the existence of rapamycin-resistant mTORC1 substrates presents a gap in our broader understanding of mTORC1-specific functions. More potent second-generation inhibitors that bind to the adenosine triphosphate (ATP) binding site of mTOR, such as Torin-1, can block both rapamycin-sensitive and -resistant mTORC1 substrates. However, these drugs also interact with mTORC2 even at low concentrations, and so their specificity is somewhat limited.

The Shokat laboratory developed a third-generation mTOR inhibitor, RapaLink1, which links rapamycin to an ATP-competitive mTOR inhibitor, MLN0128, enabling it to overcome resistance to existing first- and second-generation inhibitors (10). RapaLink1 is selective toward mTORC1 at lower doses in human glioblastoma

<sup>1</sup>University of Sydney, School of life and Environmental Sciences, Charles Perkins Centre, Sydney, New South Wales 2006, Australia. <sup>2</sup>Cellular and Molecular Pharmacology, Howard Hughes Medical Institute, University of California, San Francisco, 600 16th Street, San Francisco, CA 94143, USA. <sup>3</sup>University of Sydney, Sydney Medical School, Sydney, New South Wales 2006, Australia.

\*Corresponding author. Email: guang.yang@sydney.edu.au (G.Y.); david.james@sydney.edu.au (D.E.J.)

†These authors contributed equally to this work.

‡Present address: College of Public Health, Medical and Veterinary Sciences, Division of Tropical Health and Medicine, Department of Biomedicine and Molecular and Cell Biology, James Cook University, Douglas, Queensland, Australia.

§Present address: QIMR Berghofer Medical Research Institute, Brisbane, Queensland 4006, Australia.

||Present address: Merck Research Laboratories, 213 E Grand Ave., South San Francisco, CA 94080, USA.

cell lines (11), suggesting that it could be used as a tool to decipher different functions of mTORC1 and mTORC2. In the current study, we confirmed this notion and validated that RapaLink1 selectively inhibited mTORC1 activity but not mTORC2 at low concentrations, and this activity spanned rapamycin-sensitive and -resistant substrates in different cell types. Taking advantage of this characteristic of RapaLink1, we used it to examine the role of mTORC1 and mTORC2 in regulating different biological processes. We also compared the effects of rapamycin and RapaLink1 on starvation resistance in flies and found that, in contrast to rapamycin, which enhanced starvation resistance, complete inhibition of mTORC1 using RapaLink1 adversely affected starvation resistance. These findings extend our understanding of mTOR biology and provide insights into some of the beneficial effects of rapamycin.

## RESULTS

### RapaLink1 selectively and completely inhibits mTORC1 signaling

Although rapamycin is the most widely used mTORC1 inhibitor, it blocks the ability of mTORC1 to phosphorylate certain substrates but not others. The “high affinity” mTORC1 substrates, such as Unc-51 like autophagy activating kinase 1 (ULK1), are still phosphorylated in the presence of rapamycin, whereas the phosphorylation of the “low affinity” substrate S6K is blocked (12). This differential sensitivity is site specific and not protein specific because eukaryotic translation initiation factor 4E-binding protein 1 (4E-BP1) contains both rapamycin-sensitive (Ser<sup>65</sup>) and rapamycin-resistant (Thr<sup>37/46</sup>) sites (Fig. 1A and fig. S1A) (12). Rapamycin is highly specific for mTORC1 because it had no significant effect on the ability of mTORC2 to inhibit its bona fide substrate Akt and its downstream target NDRG1 at multiple doses of the drug (Fig. 1, B and C). In contrast, Torin-1 significantly inhibited not only mTORC1 activity but also mTORC2 activity (fig. S1B).

In contrast to Torin-1, RapaLink1 showed considerable specificity for mTORC1 at low doses without any demonstrable effects on mTORC2 activity. At low doses (3 nM), RapaLink1 selectively and almost completely blocked mTORC1 activity in human embryonic kidney (HEK) 293E cells toward both rapamycin-sensitive (S6K Thr<sup>389</sup> and 4E-BP1 Ser<sup>65</sup>) and rapamycin-resistant (4E-BP1 Thr<sup>37/46</sup> and ULK1 Ser<sup>757</sup>) sites without any demonstrable effect on mTORC2 targets (Akt Ser<sup>473</sup> and NDRG1 Thr<sup>346</sup>) (Fig. 1, B and C). We were unable to detect similar specificity for Torin-1 at any dose tested (fig. S1B). At 10 nM, RapaLink1 inhibited both mTOR complexes. We observed similar patterns in HeLa cells and 3T3-L1 adipocytes, suggesting that RapaLink1 at low concentrations represents a specific tool for studying mTORC1 biology independently of effects on mTORC2 (fig. S1, C to E). The dose-response characteristics of RapaLink1 varied among different cell lines (for example, mTORC1/2 in HeLa cells were three times as sensitive to RapaLink1 compared to HEK293E cells), and so it is crucial to perform dose analyses on a case-by-case basis.

### Prolonged treatment with low-dose RapaLink1 does not inhibit mTORC2 activity

Prolonged (>24 hours) rapamycin treatment inhibits mTORC2 activity by blocking the assembly of mTORC2 in certain cell types (13), which has been suggested as a cause for some of the adverse clinical effects of rapamycin. We next tested whether RapaLink1 has

similar properties. We used PC3 cells because they display inhibition of mTORC2 with long-term rapamycin treatment (13). PC3 cells were more sensitive to RapaLink1 than other cell types we tested (Fig. 2, A and B). Chronic treatment with 0.3 nM RapaLink1 caused substantial inhibition of mTORC1 activity without affecting mTORC2 activity, indicating that prolonged low-dose RapaLink1 treatment inhibited only mTORC1 but not mTORC2. The specificity of chronic RapaLink1 treatment on mTORC2 activity was also observed in HEK293E cells (Fig. 2, C and D), whereas rapamycin caused weak inhibition, as previously reported (13). These data demonstrate the utility of using multiple rapamycin and RapaLink1 doses to distinguish between rapamycin-resistant mTORC1, rapamycin-sensitive mTORC1, and mTORC2 substrates in multiple cell types (Fig. 2E).

### Different effects of mTOR complexes on biological processes are distinguished by RapaLink1

On the basis of the dependence of cell growth/size on mTORC1 activity (14), we assessed the effect of rapamycin, RapaLink1, and Torin-1 on cell size. Low-dose RapaLink1 (3 nM), which only inhibits mTORC1, and high-dose RapaLink1 (10 nM) and Torin-1, which inhibit both mTORC1 and mTORC2, had comparable effects on cell size, indicating that mTORC2 activity is dispensable for cell growth/size (Fig. 3A) in HEK293E cells. Although chronic rapamycin treatment caused slight inhibition of mTORC2 in HEK293E cells (Fig. 2, C and D), RapaLink1 (3 nM) and rapamycin reduced the size of cells to a similar extent (Fig. 3A), indicating that mTORC1 regulates cell size mainly through rapamycin-sensitive substrates, most likely S6K. Although the mTORC1-4E-BPs/eukaryotic translation initiation factor 4E (EIF4E) axis has also been reported to contribute to cell size regulation (15), S6K is thought to be the major downstream effector of mTORC1-driven cell growth (16, 17). For example, Ohanna *et al.* (17) reported that cell size in S6K1-deficient cells is decreased and resistant to rapamycin, which is consistent with our data.

We then assessed the effect of RapaLink1 on cell proliferation, which also depends on mTORC1 activity. Although rapamycin treatment resulted in a slight but significant inhibition of proliferation, this was less potent than the effect observed with RapaLink1 (Fig. 3B and fig. S2A), indicating that both rapamycin-sensitive and rapamycin-resistant mTORC1 substrates are involved in the regulation of cell proliferation. Again, there was no significant difference between 1 nM rapamycin (mTORC1 inhibition only) and 3 nM RapaLink1 or Torin-1 (mTORC1/2 inhibition) (Fig. 3B and fig. S2B). These data are consistent with the concept that blockage of mTORC2 is dispensable for the antiproliferative activity of mTOR inhibitors (11, 18). Furthermore, 1 nM RapaLink1 resulted in a more substantial reduction in colony size in colony formation assays than rapamycin treatment (Fig. 3C). Although 3 nM RapaLink1 and Torin-1 treatment led to a further reduction of colony size compared to 1 nM RapaLink1, this effect was very mild (Fig. 3C), indicating that mTORC1 is the main regulator of colony formation.

Another mTORC1-dependent function is autophagy. mTORC1 suppresses autophagy through phosphorylating several effectors that play key roles in both early and later stages of autophagy, including ULK1 (19–21), autophagy-related protein 13 (ATG13) (19–21), UV-radiation resistance associated gene (UVRAG) (22), death-associated protein 1 (DAP1) (23), and ATG14 (24). Although the rapamycin sensitivity of some mTORC1 substrates, such as

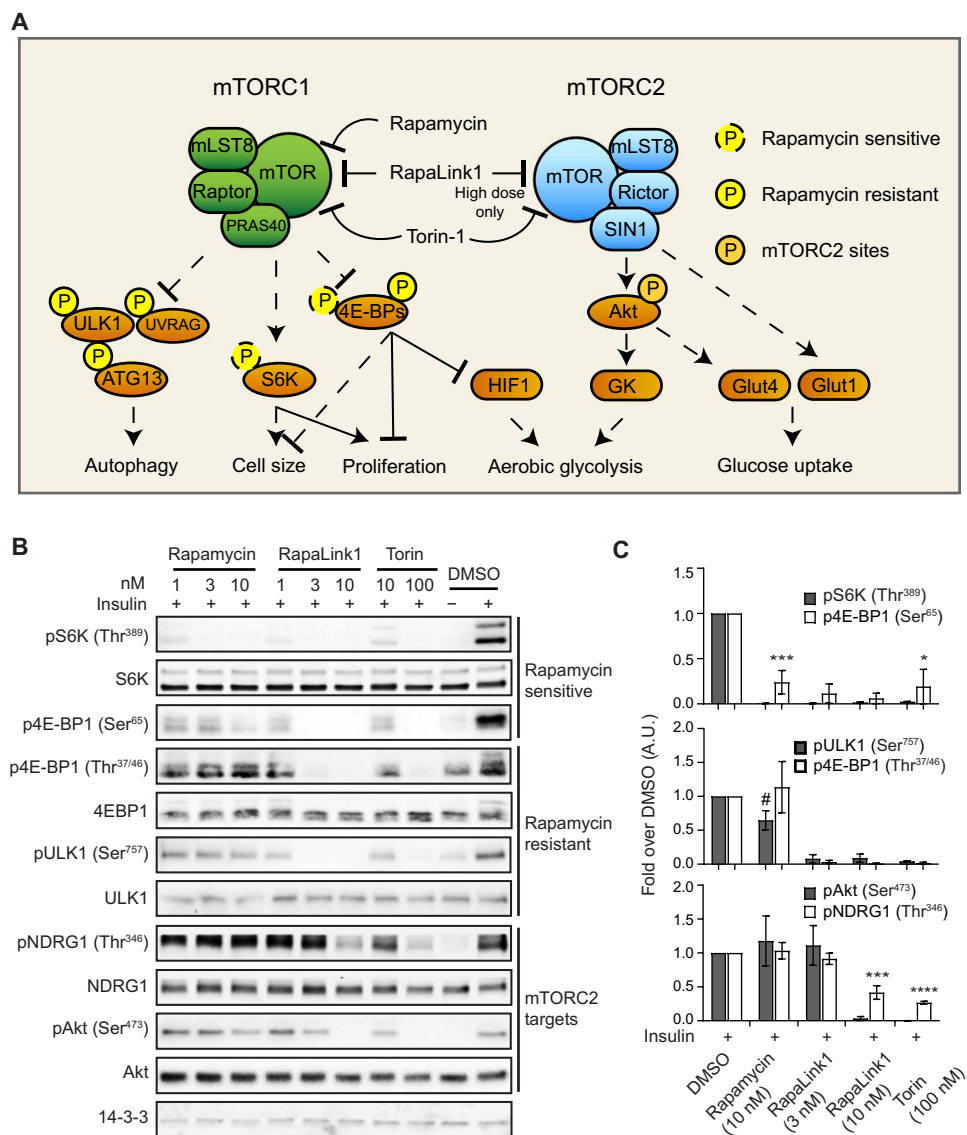


**Fig. 1. RapaLink1 selectively and completely inhibits mTORC1 signaling at low doses.** (A) Schematic shows the mTOR signaling network. (B) Western blotting analysis for mTORC1 and mTORC2 substrates on lysates from HEK293E cells treated with rapamycin, RapaLink1, and Torin-1 at the indicated doses for 4 hours under serum starvation and then stimulated with insulin (100 nM and 10 min). (C) Graph shows means  $\pm$  SEM of densitometry analyses of the Western blots in (B) normalized to total protein from three independent experiments. A.U., arbitrary units. \* $P < 0.05$ ; \*\*\* $P < 0.005$ ; \*\*\*\* $P < 0.001$ ; #, no significant difference; two-tailed Student's *t* test.

ULK1 and ATG13, is controversial (12, 25, 26), we found that the phosphorylation of Ser<sup>757</sup> in ULK1 was resistant to rapamycin in HEK293E cells (fig. S1A and Fig. 3D). Consistent with these signaling data, acute treatment with rapamycin (4 hours) had only mild effects on autophagy, whereas RapaLink1 caused a marked increase in microtubule-associated protein light chain 3-II (LC3-II) accumulation (Fig. 3D), indicating that the acute regulation of autophagy by mTORC1 is mainly mediated by rapamycin-resistant substrates. Like cell growth and size, low-dose RapaLink1 (3 nM) had identical effects to high-dose RapaLink1 (10 nM), Torin-1, and serum starvation consistent with mTORC1, but not mTORC2, being a key coordinator of the anabolic and catabolic response to various environmental and physiological stresses (27).

We next assessed the impact of RapaLink1 on aerobic glycolysis, which is reported to be regulated by both mTORC1 and mTORC2 (1, 2, 28). As expected, both rapamycin and low-dose (3 nM) RapaLink1 suppressed lactate production in HEK293E cells, a major readout of aerobic glycolysis. High-dose (10 nM) RapaLink1 and Torin-1 caused a further reduction of lactate production (Fig. 3E), indicating that unlike autophagy and cell growth, glycolysis is regulated by interplay between mTORC1 and mTORC2 activities.

Insulin plays a major role in regulating the acute uptake of glucose into adipocytes by stimulating the translocation of the glucose transporter GLUT4 to the plasma membrane and whereas mTORC2 has been implicated in this process (29, 30), the role of mTORC1 is controversial (31, 32). We reevaluated the effect of acute inhibition of mTORC1 and mTORC2 in 3T3-L1 adipocytes using RapaLink1 (Fig. 3F). Insulin-induced glucose uptake was not impaired after acute treatment with rapamycin or with low-dose (3 nM) RapaLink1. In contrast, high-dose (10 or 20 nM) RapaLink1 substantially inhibited insulin-induced glucose uptake, indicating a major role for mTORC2, but not mTORC1, in acute insulin-regulated glucose uptake. These data demonstrate that mTORC1 and mTORC2 exert differential effects on various biological processes.

### mTORC2 disruption increases the resistance of mTORC1 to RapaLink1

A problem of targeting mTOR complexes with small molecules is that a pool of free Raptor not associated with mTORC1 (33) can act as a reservoir for further mTORC1 formation by freeing mTOR associated with mTORC2. This may contribute to the development of drug resistance. We wanted to determine whether this mechanism limits the use of RapaLink1 as a specific mTORC1 inhibitor. We used 4-hydroxytamoxifen (4-OHT)-inducible Rictor knockout (iRictor) MEFs to provide a source of additional mTOR. In control [ethanol (EtOH)-treated] MEFs, 1 nM RapaLink1 significantly inhibited the phosphorylation of several major mTORC1 substrates, which was further increased at 3 nM. However, in Rictor KO (4-OHT-treated) MEFs, 1 nM RapaLink1 had no effect on the phosphorylation of 4EBP1 or ULK1, and the dose required to completely inhibit mTORC1 increased to 10 nM (Fig. 4A). Thus, disruption of mTORC2 reduced the sensitivity of mTORC1 to RapaLink1.

To further validate whether the resistance to RapaLink1 in Rictor KO cells stems from increasing mTORC1 levels, we performed

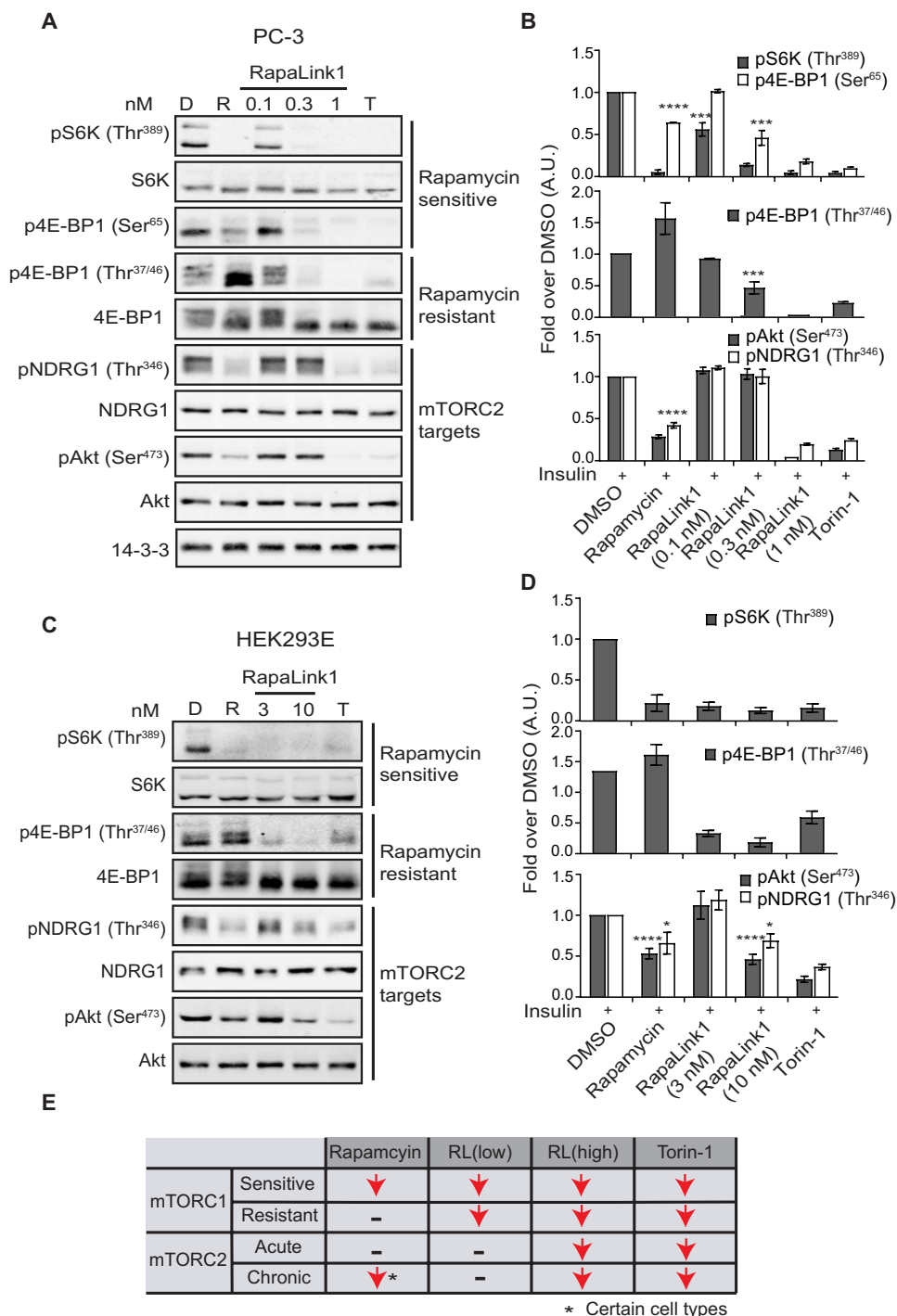


**Fig. 2. Prolonged treatment of low-dose RapaLink1 does not inhibit mTORC2 activity.** (A and C) Western blotting analysis for mTORC1 and mTORC2 substrates on lysates from PC3 (A) or HEK293E (C) cells treated with DMSO, rapamycin, Torin-1, and RapaLink1 at the indicated doses for 24 hours. Blots are representative of three (A) or four (C) independent experiments. D, DMSO; R, rapamycin; T, Torin-1. (B and D) Graph shows means  $\pm$  SEM of densitometry analyses of the Western blots in (A) and (C) normalized to total protein from three (B) or four (D) independent experiments. A.U., arbitrary units. \* $P < 0.05$ ; \*\*\* $P < 0.005$ ; \*\*\*\* $P < 0.001$ ; two-tailed Student's  $t$  test. (E) Summary of the effects of the three inhibitors on different mTOR substrates. RL, RapaLink1.

size-exclusion chromatography (SEC) to fractionate lysates from control and Rictor KO MEFs. In control MEFs, mTOR and Rictor eluted in high-molecular weight fractions ( $\sim 1.1$  to 1 MDa), consistent

with the molecular weight of mTOR complex dimers (34, 35). Unlike mTOR and Rictor, a substantial amount (39%, fractions 7 to 9) of Raptor ( $\sim 150$  kDa) was found in lower-molecular weight fractions (Fig. 4, B and C), consistent with the molecular weight of Raptor monomers, suggesting that this was the “free” Raptor pool. The ratio of free Raptor dropped from 39 to 13% in Rictor KO MEFs. Because total levels of Raptor did not substantially change (fig. S3), the altered free Raptor reflected increasing mTORC1 levels in Rictor KO MEFs, which is consistent with our hypothesis.

A similar phenomenon was observed in inducible Raptor knockout (iRapKO) MEFs (Fig. 3D). In control MEFs, 10 nM RapaLink1 was sufficient to block mTORC2 activity. However, in Raptor KO MEFs, Akt phosphorylated at Ser<sup>473</sup> was still present even up to 100 nM RapaLink1. Unlike Raptor, there was no detectable free Rictor in cells (Fig. 4B). Increased resistance of mTORC2 to RapaLink1 upon Raptor depletion is likely due to inhibition of the negative feedback loop mediated by insulin receptor substrate (IRS) (36, 37) and Grb10 (38, 39). These data suggest that disruption of one mTOR complex increases the resistance of the other mTOR complex to RapaLink1.

### Complete inhibition of TORC1 reduces starvation resistance in flies

The selective inhibition of mTORC1 activation by RapaLink1 in cell-based systems prompted us to evaluate the effect of this compound on TORC1 activity and function in vivo using *Drosophila melanogaster*. To avoid developmental effects, adult flies were raised on standard food and then given food supplemented with rapamycin or RapaLink1 for 3 days. We observed a significant reduction in phosphorylated dS6K Thr<sup>398</sup> after both rapamycin and RapaLink1 treatment, but neither of them inhibited the TORC2 substrate phosphorylated dAkt Ser<sup>505</sup> (Fig. 5A). We next evaluated the effect of this compound on starvation resistance, which has been reported to be increased by rapamycin (40). In contrast to rapamycin, RapaLink1 significantly shortened fly survival under starvation conditions (Fig. 5B).

Although the above data suggest that there are divergent effects of different classes of TORC1 substrates on starvation resistance, we wanted to ensure that this effect of RapaLink1 did not

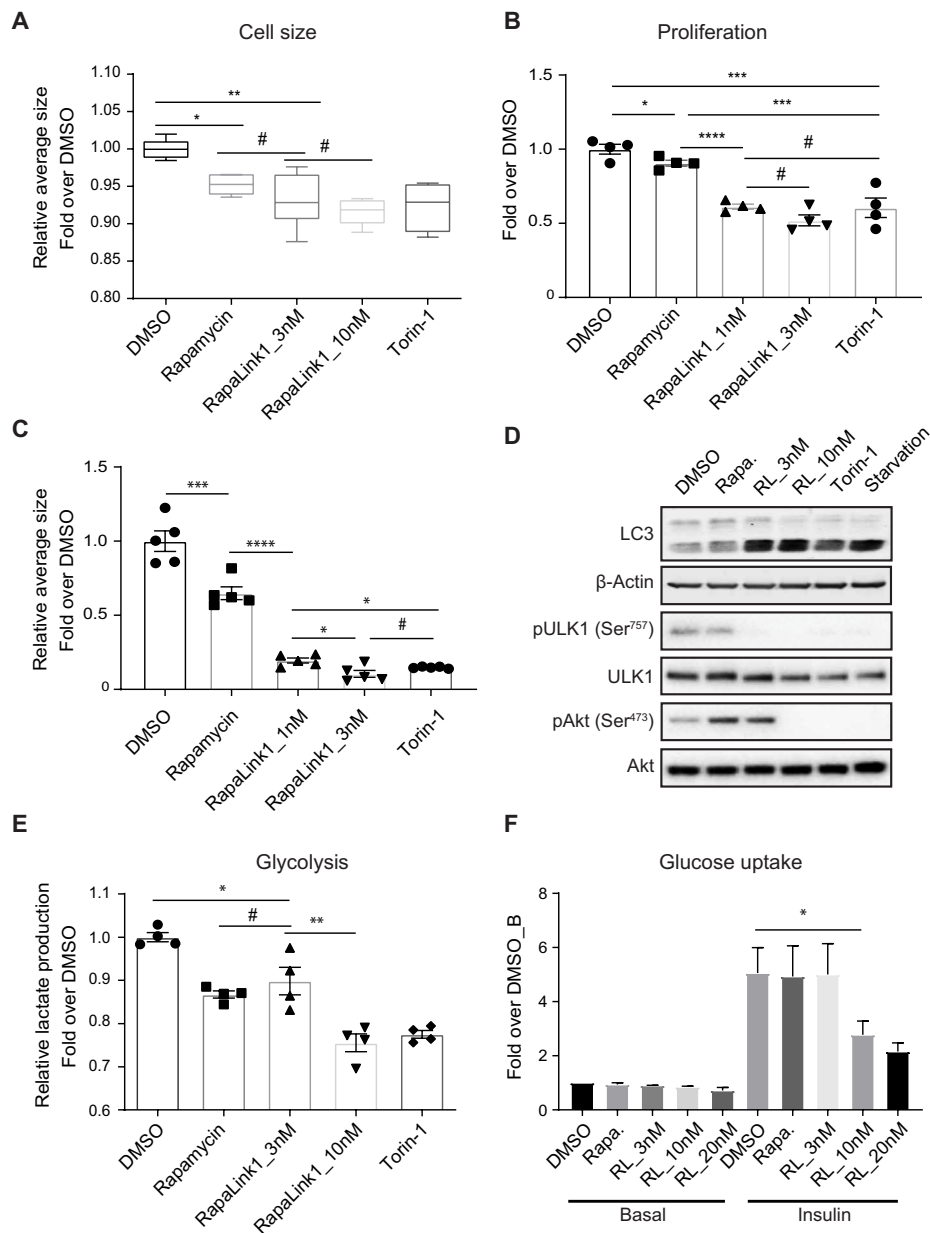


**Fig. 3. Functional outcome of mTOR inhibition by Rapalink1.** (A) Cell size analysis of HEK293E cells treated with DMSO, 10 nM rapamycin, and 100 nM Torin-1 and Rapalink1 at the indicated doses for 24 hours. Data are presented as means  $\pm$  SEM ( $*P < 0.05$ ;  $**P < 0.01$ ; #, no significant difference; two-tailed Student's *t* test,  $n \geq 4$  independent experiments). (B) Hoechst assay for cell proliferation in HeLa cells treated with DMSO, 100 nM rapamycin, and Rapalink1 at the indicated doses or 100 nM Torin-1 for 48 hours. Data are presented as means  $\pm$  SEM from four independent experiments ( $*P < 0.05$ ;  $***P < 0.005$ ;  $****P < 0.001$ ; #, no significant difference; two-tailed Student's *t* test). (C) Colony formation assay performed in HeLa cells treated with DMSO, 100 nM rapamycin, and Rapalink1 at the indicated doses or 100 nM Torin-1 for 8 days. Data are presented as means  $\pm$  SEM from five independent experiments ( $*P < 0.05$ ;  $***P < 0.005$ ;  $****P < 0.001$ ; #, no significant difference; two-tailed Student's *t* test). (D) Western blotting analysis for LC3,  $\beta$ -actin, total and phosphorylated ULK1 and Akt on lysates from HEK293E cells treated with DMSO, 100 nM rapamycin, and 100 nM Torin-1 and Rapalink1 at the indicated doses for 4 hours or serum-starved for 4 hours. Chloroquine (100  $\mu$ M) was added to the medium 30 min before harvest. Blots are representative of three independent experiments. (E) Lactate production was assessed in HEK293E cells treated with DMSO, 100 nM rapamycin, and 100 nM Torin-1 and Rapalink1 at the indicated doses for 8 hours. Data are presented as means  $\pm$  SEM from four independent experiments ( $*P < 0.05$ ;  $**P < 0.01$ ; #, no significant difference; two-tailed Student's *t* test). (F) 2-[<sup>3</sup>H]deoxyglucose uptake was quantified in 3T3-L1 adipocytes treated with DMSO, 100 nM rapamycin, and Rapalink1 at the indicated doses for 4 hours under serum starvation and then stimulated with insulin (100 nM and 20 min). Data are presented as means  $\pm$  SEM from three independent experiments ( $*P < 0.05$ , two-tailed Student's *t* test).

involve cross-reactivity with TORC2. Torin-1 inhibited both TORC1 and TORC2 in flies (Fig. 5C), and in contrast to Rapalink1, Torin-1 had only a slight inhibitory effect on starvation resistance (Fig. 5D). This result might reflect competing and divergent effects of TORC1 versus TORC2 on starvation resistance. Disruption of TORC2 by knocking down Rictor or SIN1, two key components of TORC2, significantly increased starvation resistance (figs. S4A and S4B). These data suggest that inhibition of TORC1 reduced starvation resistance. To further confirm this finding, we next examined starvation resistance in a genetically perturbed model using Raptor RNA interference (RNAi) knockdown flies. Raptor was knocked down when flies were maintained at 29°C, as confirmed by reduced phosphorylation of dS6K Thr<sup>398</sup> (Fig. 5E). As expected, depletion of Raptor significantly reduced survival under starvation conditions (Fig. 5F), demonstrating that complete inhibition of TORC1 reduces starvation resistance in flies, consistent with the effect of Rapalink1. Consistent with TORC1 inhibition, activation of TORC1 by overexpressing Rheb (fig. S4C) or knockdown of tuberous sclerosis complex 1 (TSC1) (fig. S4D) accelerated mortality under starvation conditions. These results indicate that TORC1 activation needs to be regulated within a certain range. Both hypo- and hyper-activation have an adverse effect under nutritional stress.

## DISCUSSION

Elevated mTOR activity has been linked to multiple chronic diseases and directly contributes to the process of aging (41), leading to a major exploration of mTOR inhibitors for the treatment of various diseases and as an antiaging medication. Currently, the only compounds targeting the mTOR signaling pathway for clinical application have been rapamycin and rapamycin analogs (rapalogs) and direct mTOR kinase inhibitors (second-generation inhibitors). However, treatment with rapamycin and rapalogs has only achieved modest effects in major solid tumors in the clinic (42) and produced negative side effects, including hyperglycemia, hyperlipidemia, insulin resistance, and hypertension (43, 44). The poor efficacy of this class of drug

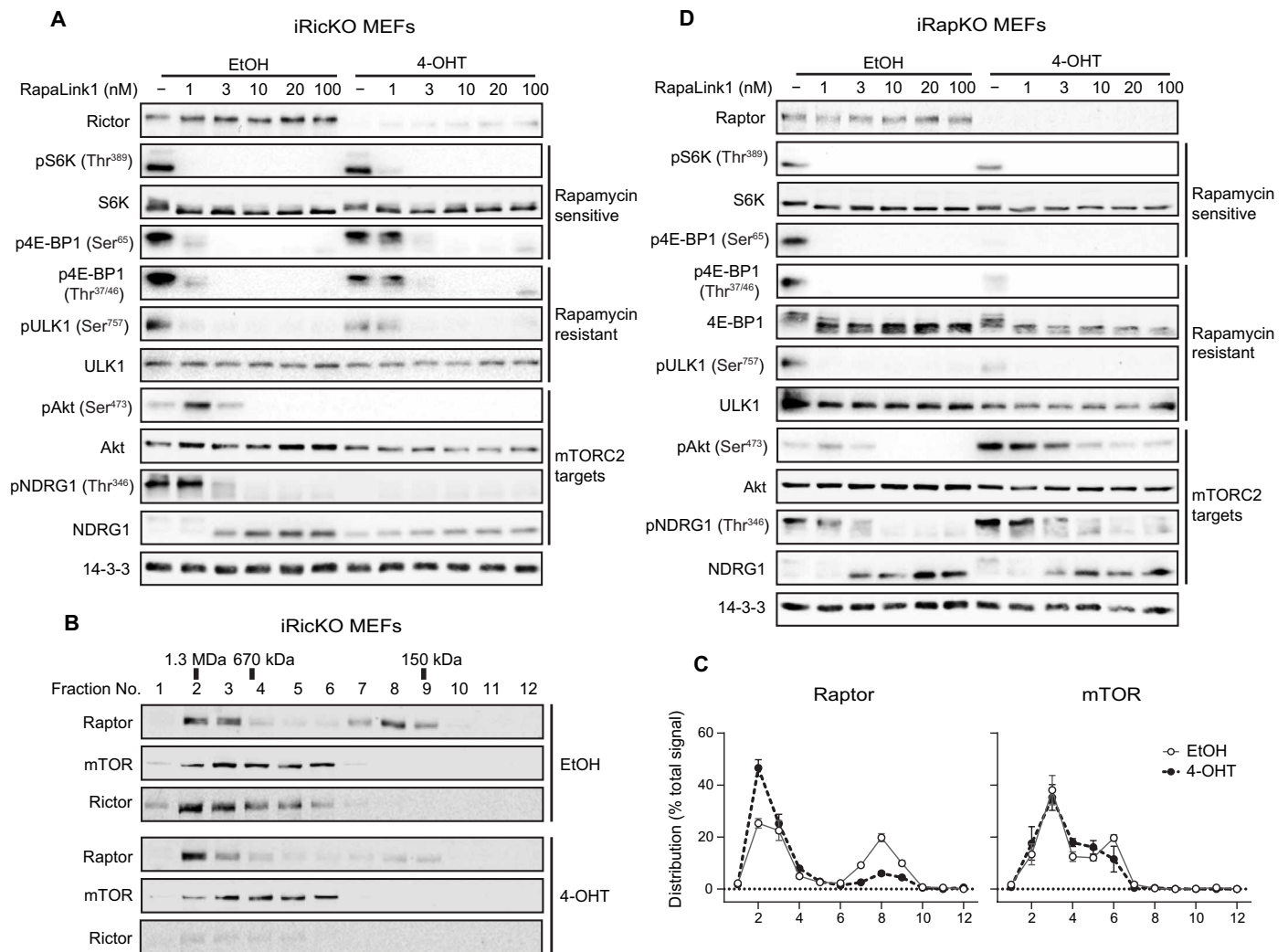


**Fig. 4. Disruption of one mTOR complex increases the resistance of the other mTOR complex to Rapamycin.** (A and D) Western blotting analysis for mTORC1 and mTORC2 substrates on lysates from iRicKO MEFs (A) or iRapKO MEFs (D) treated with EtOH or 1 mM 4-hydroxytamoxifen (4-OHT) for 3 days to induce Raptor or Rictor knockout. Treated cells were incubated with DMSO or Rapamycin at the dose indicated for 4 hours. Blots are representative of three independent experiments. (B and C) Western blotting analysis for Raptor and mTOR on lysates from iRicKO MEFs treated with EtOH or 4-OHT after size-exclusion chromatography (B) and quantification of signal per fraction normalized to total protein (C) from three independent experiments.

partially stems from incomplete mTORC1 inhibition (45, 46), and at least some of the detrimental metabolic changes result from indirect attenuation of mTORC2 signaling (47, 48). Although the second-generation inhibitors more potently inhibit mTOR activity, they tend to indiscriminately inhibit both mTORC1 and mTORC2, leading to undesirable side effects. Therefore, there is an urgent need for more specific mTORC1 inhibitors. The development of small-molecule inhibitors of mTORC1 have offered proof-of-concept evidence (49–51). Although these inhibitors overcome the disadvantages of rapamycin to varying degrees, they still have their own limitations. For example, Schreiber and colleagues identified a rapamycin analog with much greater selectivity for mTORC1 than rapamycin. However, this drug still had minimal effects on the rapamycin-resistant functions of mTORC1 as an FK506-binding protein 12 (FKBP12)-dependent rapalog (49). Navitor Pharmaceuticals have developed two compounds that indirectly inhibit mTORC1 through targeting Rheb (50) and Glut1 (51). Although these two drugs can inhibit the full functions of

mTORC1, they may cause side effects of an unknown nature because of affecting mTORC1-independent functions of Rheb (52) and Glut1.

The third-generation mTOR inhibitor Rapamycin was initially designed to overcome resistance to existing first- and second-generation inhibitors, because it can interact with the FRB domain of mTOR by binding to FKBP12, and also to simultaneously bind the kinase domain of mTOR acting as an ATP-competitive inhibitor (10). In this study, we showed that, at a low dose, Rapamycin selectively and completely inhibited mTORC1 activity, including both rapamycin-sensitive and -resistant substrates (Fig. 1, B and C). Rapamycin had a more potent effect than rapamycin on several key pathways that are linked to human diseases and aging, including cell proliferation, autophagy, and glycolysis (Fig. 3, B, D, and E). Furthermore, unlike rapamycin, long-term treatment with low-dose Rapamycin did not inhibit mTORC2 either in cell lines (Fig. 2, A to D) or in vivo [Fig. 5A, (11)]. This advantage of Rapamycin enhances its potential utility in the clinic.

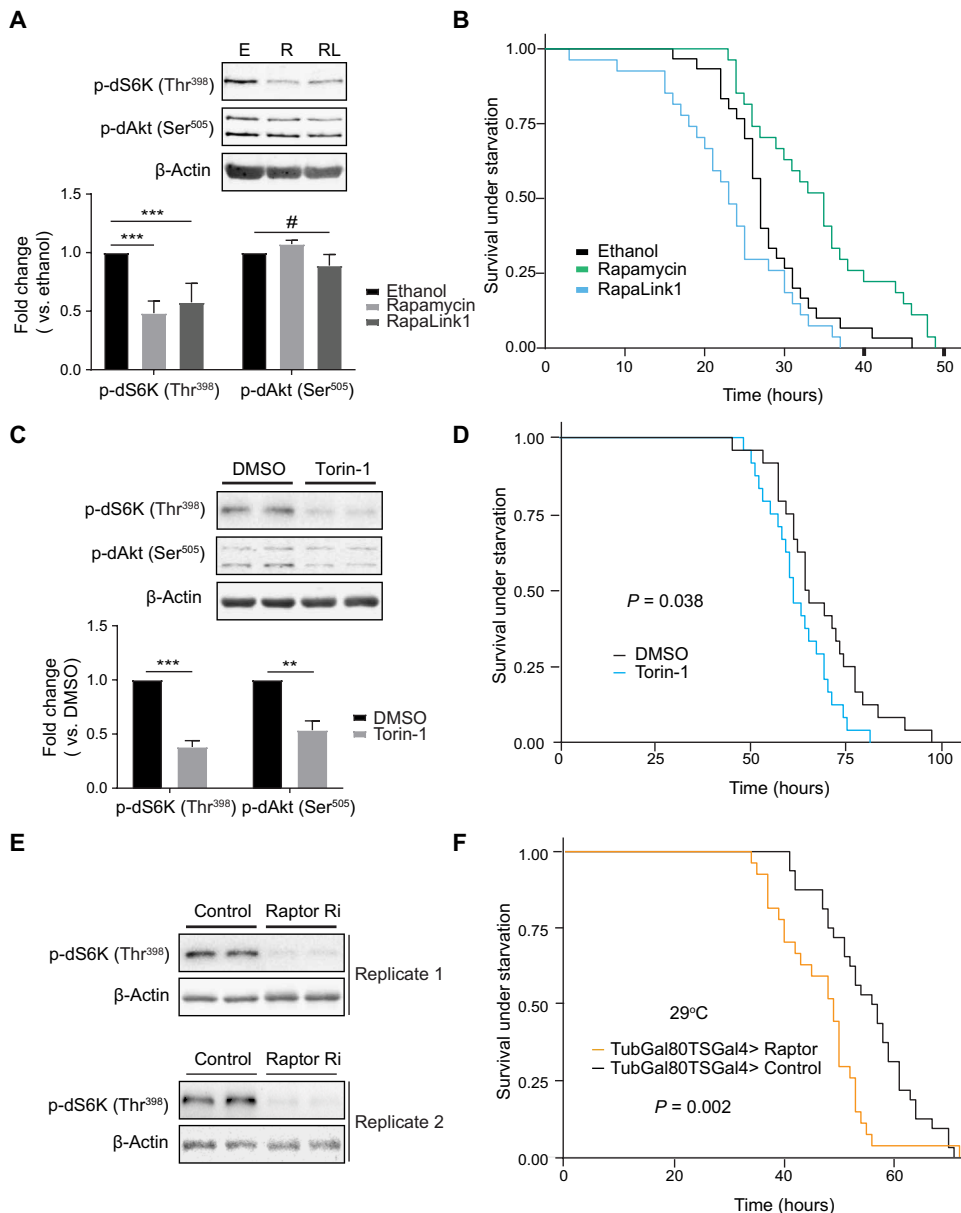


**Fig. 5. Complete inhibition of TORC1 reduces starvation resistance in flies.** (A and B) Mated adult female flies were fed with EtOH (E), 200  $\mu$ M rapamycin (R), or 6  $\mu$ M RapaLink1 (RL) for 3 days. The heads and thoraxes of five flies were subjected to Western blotting for the indicated proteins, which was quantified (A). The results are shown as means  $\pm$  SEM from four independent experiments (\*\*\* $P$  < 0.005; #, no significant difference; two-tailed Student's  $t$  test). The remaining flies were placed into *Drosophila* activity monitor system (DAMS) tubes with 2% agar for continuous monitoring (B). The  $P$  values for rapamycin and RapaLink1 treatments are 0.002 and 0.052, respectively (log-rank test compared to EtOH treatment,  $n$  = 16 for each group). (C and D) Mated adult female flies were fed with DMSO or 10  $\mu$ M Torin-1 for 3 days. The heads and thoraxes of five flies were subjected to Western blotting for the indicated proteins, which was quantified (C). The results are shown as means  $\pm$  SEM from three independent experiments (\*\* $P$  < 0.01, \*\*\* $P$  < 0.005, two-tailed Student's  $t$  test). The remaining flies were placed into DAMS tubes with 2% agar for continuous monitoring. Log-rank test was performed ( $n$  = 16 for each group) (D). (E and F) Mated *tubulin-GAL80<sup>ts</sup>; tubulin-GAL4 UAS-Raptor<sup>HMS02306</sup>* RNAi or control adult female flies were raised at 18°C and shifted to 29°C for 3 days. The heads and thoraxes of five females were subjected to Western blotting for the indicated proteins from two independent experiments (E). Sixteen females per genotype were placed into DAMS tubes with 2% agar for continuous monitoring. Log-rank test was performed (F).

At higher doses, RapaLink1 did inhibit mTORC2 (Fig. 1B) in different cell types but at variable effective doses (fig. S1, C to E). This special characteristic makes RapaLink1 unique from any other

mTOR inhibitors and to be a powerful experimental tool to delineate distinct functions of mTORC1 and mTORC2. Using RapaLink1, we determined that (i) mTOR mainly regulated cell growth/size and autophagy through mTORC1; (ii) only mTORC2 acutely affected insulin-induced glucose uptake; and (iii) both complexes played roles in aerobic glycolysis (Fig. 3, A, D, E, and F). By comparing rapamycin and RapaLink1, we could discriminate between rapamycin-sensitive and rapamycin-resistant functions of mTORC1 (Fig. 2E). A phosphoproteomics analysis using rapamycin- or RapaLink1-treated cells will resolve the full repertoire of rapamycin-sensitive and rapamycin-resistant mTORC1 substrates. However, the sensitivity of different cell types to RapaLink1 varied considerably (Figs. 1B and 2, A to D, and fig. S1, B and C). In HEK293E cells, 3 nM RapLink1 caused substantial inhibition of mTORC1 activity without affecting mTORC2 activity, whereas in PC3 cells, the dose required to achieve the same effect was 10-fold less (0.3 nM). Therefore, it is important to perform dose analyses before starting the experiments.

The narrow window between mTORC1 and mTORC2 inhibition is the major disadvantage of RapaLink1. In most cases, the selectivity for mTORC1 compared to mTORC2 inhibition is about threefold (Figs. 1B and 2, A to D, and fig. S1, B and C). Therefore, the concentration of this drug needs to be chosen to selectively inhibit mTORC1. Although the narrow inhibition window may limit the application of RapaLink1 in vivo, the selectivity on TORC1 has been validated in both fly (Fig. 5A) and mouse, where RapaLink1 (4 mg/kg) inhibits the phosphorylation of S6 and 4EBP1, but not that of Akt Ser<sup>473</sup> in multiple tissues (11). The mTORC1 selectivity of RapaLink1 in other model organisms or even humans needs to be further investigated. Furthermore, chronic treatment of RapaLink1 still causes weight loss, glucose intolerance, and liver toxicity in mice, similar to what was previously reported for rapamycin (53), indicating that these side effects are likely to stem from inhibition of rapamycin-sensitive substrates. We further observed that

disruption of one mTOR complex reduced the sensitivity of the other complex to RapaLink1 through different mechanisms (Fig. 4, A and D). This phenomenon likely underpins the cell type specificity of

dose-response effects of RapaLink1 (fig. S1, C to E) in that different cell types may express different amounts of these two mTOR complexes.

The most exciting but unexpected finding was that RapaLink1 had opposing effects on starvation resistance compared to rapamycin in flies (Fig. 5A). Although we were unable to evaluate the effects of RapaLink1 on rapamycin-resistant substrates in flies because of lack of suitable antibodies, a previous study demonstrated that RapaLink1 substantially reduced phosphorylation of 4EBP1 Thr<sup>37/46</sup> in multiple mouse tissues (11). Consistent with this finding, we also showed that RapaLink1 inhibited phosphorylation of both rapamycin-sensitive and -resistant mTORC1 substrates at the same concentration in multiple cell types. Therefore, we are confident that it could completely inhibit TORC1 in flies. Our further validation using Torin-1 and Raptor RNAi flies confirmed that depletion of TORC1 activity shortened rather than extended survival under starvation conditions (Fig. 5, B and C). These unexpected findings could explain some controversial results from previous studies. For example, rapamycin has life-extending properties and promotes starvation resistance in multiple model organisms (40). However, TOR (dTOR) mutant flies, where both mTORC1 and mTORC2 functions are impaired, show extended life span without effects on starvation resistance (54). On the basis of our work, we predict that this reflects opposing effects of mTORC1 and mTORC2 on starvation resistance such that when both are disrupted simultaneously, the outcome will be determined by the aggregate contribution of the two competing pathways.

The beneficial effects of rapamycin on starvation resistance have been thought to stem from inhibition of TORC1-mediated protein synthesis or up-regulation of autophagy. However, this may not be the case because constitutive activation of protein synthesis or blockage of autophagy overcomes the beneficial effects of rapamycin on life span but not on starvation resistance in flies (40). Another possibility is that rapamycin treatment affects fat metabolism and energy reserves, which may promote starvation resistance. Two groups have reported that rapamycin increases triglyceride stores (40, 55), an effect that is partially dependent on the activity of 4E-BP (55). Furthermore, 4E-BP can function as a metabolic brake during starvation, because 4E-BP null flies burn fat quicker and die faster than control flies in periods of starvation (55). Torin-1 treatment or Raptor depletion reduces the total levels of 4E-BP1 in human foreskin fibroblasts (56). These findings raise the possibility that the opposing effect of RapaLink1 on starvation resistance arises from decreasing the total levels of 4E-BP through the rapamycin-resistant function of TORC1. Further experiments need to be performed to validate this hypothesis. In summary, mTORC1 has multiple targets. Inhibiting some of them (rapamycin targets) promotes starvation resistance, whereas inhibiting all of them (RapaLink1 targets) impairs starvation resistance. This calls for a reevaluation of the field with particular attention to the role of these different classes of mTORC1 dependent substrates.

## MATERIALS AND METHODS

### Reagents and antibodies

Dulbecco's modified Eagle's medium (DMEM) and L-GlutaMAX were from Gibco. Fetal bovine serum (FBS) was from Hyclone Laboratories. Insulin, dimethyl sulfoxide (DMSO), and chloroquine were from Sigma-Aldrich. Rapamycin was from LC Laboratories.

Torin-1 was from Tocris Bioscience. RapaLink1 was provided by K.M.S. All primary antibodies were diluted 1:1000 in dilution buffer containing 5% bovine serum albumin (BSA), 0.1% Tween 20, and 0.02% NaN<sub>3</sub> in tris-buffered saline (TBS) buffer [1.2% tris-HCl (pH 7.4) and 8.7% NaCl]. Pan 14-3-3 polyclonal rabbit antibodies were from Santa Cruz Biotechnology. All other primary antibodies were from Cell Signaling Technology. The anti-mouse horseradish peroxidase (HRP)-conjugated secondary antibody was from GE Healthcare (Buckinghamshire, UK), and the anti-rabbit HRP-conjugated secondary antibody was from Jackson ImmunoResearch. Polyvinylidene difluoride membrane was purchased from Millipore (Billerica, MA). In some cases, IRDye 700- or 800-conjugated secondary antibodies were used, and these were obtained from Rockland Immunochemicals.

### Cell culture

HeLa, C2C12, and HEK293E cells were maintained in DMEM (4.5 g of glucose/liter) with 2 mM L-GlutaMAX and 10% FBS. iRapKO MEFs and iRicKO MEFs were cultured in DMEM with 10% FBS, 2 mM L-GlutaMAX, nonessential amino acids, and 1 mM sodium pyrophosphate. 4-OHT induction of Raptor or Rictor knockout was performed as previously described (57). 3T3-L1 fibroblasts (a gift from H. Green, Harvard Medical School) were grown in DMEM containing 10% FBS and 2 mM L-GlutaMAX in 10% CO<sub>2</sub> at 37°C. For differentiation into adipocytes, cells were grown to confluence and then treated with DMEM/FBS containing insulin (4 µg/ml), 0.25 mM dexamethasone, 0.5 mM 3-isobutyl-1-methylxanthine, and D-biotin (100 ng/ml). After 72 hours, the differentiation medium was replaced with fresh FBS/DMEM containing insulin (4 µg/ml) and D-biotin (100 ng/ml) for a further 3 days and then replaced with fresh FBS/DMEM. Adipocytes were refed with FBS/DMEM every 48 hours and used for experiments between 9 and 12 days after the initiation of differentiation. These cells were routinely tested for mycoplasma.

### Western blotting

Proteins were separated by SDS-polyacrylamide gel electrophoresis (SDS-PAGE) and transferred to polyvinylidene difluoride membranes. The membranes were incubated in a blocking buffer containing 5% skim milk in TBS and immunoblotted with the relevant antibodies overnight at 4°C in the blocking buffer containing 5% BSA and 0.1% Tween in TBS buffer. After incubation, the membranes were washed and incubated with HRP-labeled secondary antibodies for 1 hour and then detected by SuperSignal West Pico chemiluminescent substrate. In some cases, IRDye 700- or 800-conjugated secondary antibodies were used and then scanned at the 700- and 800-nm channels using an Odyssey IR imager.

### Colony formation assay

HeLa cells were seeded into six-well plates (300 cells per well) and left for 8 to 12 days until formation of visible colonies. Colonies were washed with phosphate-buffered saline (PBS) and fixed with 10% acetic acid/10% methanol for 20 min and then stained with 0.4% crystal violet in 20% EtOH for 20 min. After staining, the plates were washed and air-dried, and colony numbers were counted. Average size of colonies was measured using ImageJ. Briefly, colonies in each well were identified using the Trainable Weka Segmentation tool (58). After segmentation, images were transformed to 8-bit gray scale, followed by applying a threshold for each well

individually and colony analysis. Plating efficiency (PE) in untreated cells was 0.46 (PE =  $N$  of colonies/ $N$  of cells plated). The area and number of colonies were normalized against untreated cells.

### Hoechst assay

The Hoechst assays for cell proliferation were performed as described previously (59). Briefly, HeLa cells were seeded into 96-well plates (3000 cells per well) and fed overnight in DMEM containing 10% FBS and 2 mM GlutaMAX. Cells were then treated with DMSO, 100 nM rapamycin, and 1 or 3 nM RapaLink1 for 2 days. Medium was aspirated, and the plate was frozen at  $-80^{\circ}\text{C}$ . Plates were then thawed at room temperature, and 100  $\mu\text{l}$  of water was added per well before freezing once more at  $-80^{\circ}\text{C}$ . Plates were thawed, followed by the addition of 100  $\mu\text{l}$  of Hoechst-33258 solution containing Hoechst-33258 (10  $\mu\text{g}/\text{ml}$ ) in TNE buffer [10 mM tris-HCl (pH 7.4), 2 M NaCl, and 1 mM EDTA]. The fluorescence was measured at fluorescence excitation (FEx) = 360 nm and fluorescence emission (FEm) = 440 nm.

### Cell size determinations

HEK293E cells were treated with DMSO, 100 nM rapamycin, 100 nM Torin-1, and RapaLink1 (3 and 10 nM) for 24 hours. To measure cell size, cells were harvested by trypsinization and diluted in PBS, and then 5000 to 25,000 cells were subjected to cell size analysis on Countess II (Thermo Fisher Scientific).

### Measurement of lactate production

Media lactate levels were assayed enzymatically as described previously (60). Briefly, the assay buffer was 1 M glycine (pH 9.2), 0.4 M hydrazine sulfate in 1 M NaOH, and 2.5 mM EDTA, adjusted to pH 9.2 with NaOH before the addition of 4 mM nicotinamide adenine dinucleotide phosphate ( $\text{NAD}^+$ ) and lactate dehydrogenase (2 U/ml; Roche Applied Science). An aliquot of medium sample was diluted in water (100  $\mu\text{l}$  total) and incubated with 100  $\mu\text{l}$  of assay buffer in a microplate format. Reactions were protected from light and incubated at room temperature for at least 1 hour, after which the absorbance of NADH (the reduced form of  $\text{NAD}^+$ ) was measured at 340 nm. Reactions with medium samples without lactate dehydrogenase were included as a negative control. Lactate levels were quantified using a standard curve of lactate added to the naive culture medium.

### 2-Deoxyglucose uptake assays

After 4 hours of serum starvation in DMEM/0.2% BSA/1% GlutaMAX with DMSO or inhibitors (100 nM rapamycin and 3, 10, and 20 nM RapaLink1), cells were washed and incubated in prewarmed Krebs-Ringer phosphate buffer containing 0.2% BSA (Bovostar, Bovogen) [Krebs-Ringer Phosphate Hepes (KRPH) buffer; 0.6 mM  $\text{Na}_2\text{HPO}_4$ , 0.4 mM  $\text{NaH}_2\text{PO}_4$ , 120 mM NaCl, 6 mM KCl, 1 mM  $\text{CaCl}_2$ , 1.2 mM  $\text{MgSO}_4$ , and 12.5 mM Hepes (pH 7.4)]. Cells were stimulated with 100 nM insulin for 20 min. To determine nonspecific glucose uptake, 25  $\mu\text{M}$  cytochalasin B (EtOH, Sigma-Aldrich) was added to the wells before the addition of 2- $^3\text{H}$ deoxyglucose (2-DOG) (PerkinElmer). During the final 5 min, 2-DOG (0.25  $\mu\text{Ci}$ , 50  $\mu\text{M}$ ) was added to cells to measure steady-state rates of 2DOG uptake. After three washes with ice-cold PBS, cells were solubilized in PBS containing 1% (v/v) Triton X-100. Tracer uptake was quantified by liquid scintillation counting and data-normalized for protein content. Data were further normalized to maximal insulin stimulation of control cells set to 100%.

### Size-exclusion chromatography

iRicKO MEFs treated with EtOH or 4-OHT were lysed in ice-cold CHAPS-containing buffer [50 mM Na-Hepes, 100 mM NaCl, 2 mM  $\text{MgCl}_2$ , 2 mM dithiothreitol (DTT), and 0.3% CHAPS, complete EDTA-free protease inhibitors]. The lysate was passaged six times on ice through a 1-ml syringe with a 22- and 27-gauge needle and cleared by ultracentrifugation at 12,000g for 20 min at  $4^{\circ}\text{C}$ . The cleared lysates were normalized to a protein concentration of 4 mg/ml in the CHAPS buffer. The lysates (500  $\mu\text{l}$  per sample) were filtered to remove large particles through 0.45- $\mu\text{m}$  spin filters (Millipore Ultrafree-MC) at 12,000g for 1 min at  $4^{\circ}\text{C}$ . Using a Thermo Dionex BioRS UHPLC system, each sample kept at  $4^{\circ}\text{C}$  was injected (350  $\mu\text{l}$  per sample) onto an Agilent AdvanceBio SEC column (7.8  $\times$  300 mm, 300A pores, 2.7- $\mu\text{m}$  particles). Before separations, the column was cooled to  $5^{\circ}\text{C}$  and preequilibrated with 10 column volumes of SEC running buffer (0.3% CHAPS, 50 mM Na-Hepes, 100 mM NaCl, 2 mM  $\text{MgCl}_2$ , and 2 mM DTT). The flow rate was 0.5 ml/min, and 12 fractions were collected from retention time 8.5 to 14.5 min with a total run time per sample of 45 min. The fractions in the SEC running buffer were diluted into SDS-PAGE sample buffer, and equal fraction volumes were loaded for Western blotting.

### Drosophila stocks and procedures

The following stocks were obtained from the Bloomington *Drosophila* stock center (Indiana University, Indiana, USA): UAS-Rheb (#9688), UAS-Raptor RNAi HMS02306 (#41912), UAS-Rictor RNAi (HMS01588, #36699), UAS-SIN1 RNAi (HMS01565, #36677), UAS-TSC1 RNAi (JF01484, #31039), TRIP RNAi control stocks (#36306 and #3607), and *ubiquitous-GAL4* (#32551). The following flies were also used:  $W^{1118}$  (Vienna *Drosophila* Resource Centre, Vienna, Austria, #6000), UAS-mouseCD8::GFP (Kyoto Stock Center, Kyoto, Japan, #108068), and *tubulin-GAL80ts;tubulin-GAL4* (a gift from E. Havula, University of Sydney). Flies were maintained at standard temperature, humidity, and 12-hour light/dark cycle unless otherwise stated. Flies were fed a standard diet of yeast and sugar.

The GAL4-UAS system was used for overexpression and knock-down experiments. Twenty *ubi-GAL4* virgin females were crossed with 5 to 10 males carrying a UAS-RNAi, control, or UAS overexpression for 3 days. Newly emerged adult progeny with the correct genotype were mated for 48 hours, and females were selected for experiments.

For temperature-sensitive experiments, *tub-GAL80<sup>ts</sup>*; *tub-Gal4* females were crossed with UAS-Raptor RNAi 41912 males at  $18^{\circ}\text{C}$  for 5 days to ensure embryo survival. Flies were raised at  $18^{\circ}\text{C}$  to repress the expression of *tub-GAL4* and RNAi expression. Mated adult females were collected and incubated at  $29^{\circ}\text{C}$  for 3 days to inactivate *tub-Gal80<sup>ts</sup>* and activate *tub-GAL4* and RNAi expression. Females were then removed from  $29^{\circ}\text{C}$  for Western blotting or starvation resistance assays.

Drugs were administered into the fly food (2.5% sugar, 5% yeast, and 1% agar). Briefly, sugar and yeast were added to boiled agar on a hot plate and left to cool to  $55^{\circ}\text{C}$  with stirring. Fly food (2 ml) was added into individual vials, where stock solutions of rapamycin, RapaLink1, and Torin-1 were diluted into cooled fly food (at  $55^{\circ}\text{C}$ ) for a final concentration of 200, 6, and 10  $\mu\text{M}$ , respectively. The same volume of EtOH was added as a vehicle control. Groups of 16 mated female flies were added to each vial for 3 days. Flies were then collected for Western blotting or assayed for starvation resistance.

We used the *Drosophila* activity monitoring system (Trikinetics) (61) to assay survival during starvation. Sixteen mated female flies were placed into individual *Drosophila* activity monitor system (DAMS) tubes sealed with 2% agar on one end and a cotton plug on the other end. Monitors were kept at 25°C/65% humidity with 12-hour light/dark cycles for all experiments. Activity was monitored every 5 min, and death was counted as a complete absence of activity lasting longer than 5 min. The median starvation resistance was derived with the survival and survminor packages (R).

To prepare samples for Western blotting, mated adult female flies were anesthetized with CO<sub>2</sub>. A scalpel was used to quickly separate the head and thorax from the abdomen. Heads and thoraxes were then flash-frozen in liquid N<sub>2</sub>.

## SUPPLEMENTARY MATERIALS

[www.science.org/doi/10.1126/scisignal.abe0161](http://www.science.org/doi/10.1126/scisignal.abe0161)

Figs. S1 to S4

[View/request a protocol for this paper from Bio-protocol.](#)

## REFERENCES AND NOTES

- R. A. Saxton, D. M. Sabatini, mTOR signaling in growth, metabolism, and disease. *Cell* **169**, 361–371 (2017).
- I. Ben-Sahra, B. D. Manning, mTORC1 signaling and the metabolic control of cell growth. *Curr. Opin. Cell Biol.* **45**, 72–82 (2017).
- Z. Zhu, C. Yang, A. Iyaswamy, S. Krishnamoorthi, S. G. Sreenivasamurthy, J. Liu, Z. Wang, B. C. Tong, J. Song, J. Lu, K. H. Cheung, M. Li, Balancing mTOR signaling and autophagy in the treatment of Parkinson's disease. *Int. J. Mol. Sci.* **20**, 728 (2019).
- E. Jacinto, V. Facchinetti, D. Liu, N. Soto, S. Wei, S. Y. Jung, Q. Huang, J. Qin, B. Su, SIN1/MIP1 maintains rictor-mTOR complex integrity and regulates Akt phosphorylation and substrate specificity. *Cell* **127**, 125–137 (2006).
- A. Kumar, J. C. Lawrence Jr., D. Y. Jung, H. J. Ko, S. R. Keller, J. K. Kim, M. A. Magnuson, T. E. Harris, Fat cell-specific ablation of rictor in mice impairs insulin-regulated fat cell and whole-body glucose and lipid metabolism. *Diabetes* **59**, 1397–1406 (2010).
- C. F. Bentzinger, K. Romanino, D. Cloetta, S. Lin, J. B. Mascarenhas, F. Oliveri, J. Xia, E. Casanova, C. F. Costa, M. Brink, F. Zorzato, M. N. Hall, M. A. Ruegg, Skeletal muscle-specific ablation of raptor, but not of rictor, causes metabolic changes and results in muscle dystrophy. *Cell Metab.* **8**, 411–424 (2008).
- P. L. Lee, Y. Tang, H. Li, D. A. Guertin, Raptor/mTORC1 loss in adipocytes causes progressive lipodystrophy and fatty liver disease. *Mol. Metab.* **5**, 422–432 (2016).
- A. L. Kearney, K. C. Cooke, D. M. Norris, A. Zadoorian, J. R. Krycer, D. J. Fazakerley, J. G. Burchfield, D. E. James, Serine 474 phosphorylation is essential for maximal Akt2 kinase activity in adipocytes. *J. Biol. Chem.* **294**, 16729–16739 (2019).
- C. H. Aylett, E. Sauer, S. Imseng, D. Boehringer, M. N. Hall, N. Ban, T. Maier, Architecture of human mTOR complex 1. *Science* **351**, 48–52 (2016).
- V. S. Rodrik-Outmezguine, M. Okaniwa, Z. Yao, C. J. Novotny, C. McWhirter, A. Banaji, H. Won, W. Wong, M. Berger, E. de Stanchina, D. G. Barratt, S. Cosulich, T. Klinowska, N. Rosen, K. M. Shokat, Overcoming mTOR resistance mutations with a new-generation mTOR inhibitor. *Nature* **534**, 272–276 (2016).
- Q. Fan, O. Aksoy, R. A. Wong, S. Ilkhanizadeh, C. J. Novotny, W. C. Gustafson, A. Y. Truong, G. Cayan, E. F. Simonds, D. Haas-Kogan, J. J. Phillips, T. Nicolaidis, M. Okaniwa, K. M. Shokat, W. A. Weiss, A kinase inhibitor targeted to mTORC1 drives regression in glioblastoma. *Cancer Cell* **31**, 424–435 (2017).
- S. A. Kang, M. E. Pacold, C. L. Cervantes, D. Lim, H. J. Lou, K. Ottina, N. S. Gray, B. E. Turk, M. B. Yaffe, D. M. Sabatini, mTORC1 phosphorylation sites encode their sensitivity to starvation and rapamycin. *Science* **341**, 1236566 (2013).
- D. D. Sarbassov, S. M. Ali, S. Sengupta, J. H. Sheen, P. P. Hsu, A. F. Bagley, A. L. Markhard, D. M. Sabatini, Prolonged rapamycin treatment inhibits mTORC2 assembly and Akt/PKB. *Mol. Cell* **22**, 159–168 (2006).
- M. S. Yoon, The role of mammalian target of rapamycin (mTOR) in insulin signaling. *Nutrients* **9**, 1176 (2017).
- D. C. Fingar, S. Salama, C. Tsou, E. Harlow, J. Blenis, Mammalian cell size is controlled by mTOR and its downstream targets S6K1 and 4EBP1/eIF4E. *Genes Dev.* **16**, 1472–1487 (2002).
- B. Magnuson, B. Ekim, D. C. Fingar, Regulation and function of ribosomal protein S6 kinase (S6K) within mTOR signalling networks. *Biochem. J.* **441**, 1–21 (2012).
- M. Ohanna, A. K. Sobering, T. Lapointe, L. Lorenzo, C. Praud, E. Petroulakis, N. Sonenberg, P. A. Kelly, A. Sotiropoulos, M. Pende, Atrophy of S6K1<sup>-/-</sup> skeletal muscle cells reveals distinct mTOR effectors for cell cycle and size control. *Nat. Cell Biol.* **7**, 286–294 (2005).
- J. Atkin, L. Halova, J. Ferguson, J. R. Hitchin, A. Lichawska-Cieslar, A. M. Jordan, J. Pines, C. Wellbrock, J. Petersen, Torin1-mediated TOR kinase inhibition reduces Wee1 levels and advances mitotic commitment in fission yeast and HeLa cells. *J. Cell Sci.* **127**, 1346–1356 (2014).
- I. G. Ganley, D. H. Lam, J. Wang, X. Ding, S. Chen, X. Jiang, ULK1-ATG13-FIP200 complex mediates mTOR signaling and is essential for autophagy. *J. Biol. Chem.* **284**, 12297–12305 (2009).
- N. Hosokawa, T. Hara, T. Kaizuka, C. Kishi, A. Takamura, Y. Miura, S. Iemura, T. Natsume, K. Takehana, N. Yamada, J. L. Guan, N. Oshiro, N. Mizushima, Nutrient-dependent mTORC1 association with the ULK1-Atg13-FIP200 complex required for autophagy. *Mol. Biol. Cell* **20**, 1981–1991 (2009).
- C. H. Jung, C. B. Jun, S. H. Ro, Y. M. Kim, N. M. Otto, J. Cao, M. Kundu, D. H. Kim, ULK-Atg13-FIP200 complexes mediate mTOR signaling to the autophagy machinery. *Mol. Biol. Cell* **20**, 1992–2003 (2009).
- Y.-M. Kim, C. H. Jung, M. Seo, E. K. Kim, J.-M. Park, S. S. Bae, D.-H. Kim, mTORC1 phosphorylates UVRAG to negatively regulate autophagosome and endosome maturation. *Mol. Cell* **57**, 207–218 (2014).
- I. Koren, E. Reem, A. Kimchi, DAP1, a novel substrate of mTOR, negatively regulates autophagy. *Curr. Biol.* **20**, 1093–1098 (2010).
- H. X. Yuan, R. C. Russell, K. L. Guan, Regulation of PIK3C3/VPS34 complexes by mTOR in nutrient stress-induced autophagy. *Autophagy* **9**, 1983–1995 (2013).
- C. Puente, R. C. Hendrickson, X. Jiang, Nutrient-regulated phosphorylation of ATG13 inhibits starvation-induced autophagy. *J. Biol. Chem.* **291**, 6026–6035 (2016).
- J. Kim, M. Kundu, B. Viollet, K. L. Guan, AMPK and mTOR regulate autophagy through direct phosphorylation of Ulk1. *Nat. Cell Biol.* **13**, 132–141 (2011).
- M. Paquette, L. El-Houjeiri, A. Pause, mTOR pathways in cancer and autophagy. *Cancers* **10**, 18 (2018).
- H. Chi, Sin1-mTORC2 signaling drives glycolysis of developing thymocytes. *J. Mol. Cell Biol.* **11**, 91–92 (2019).
- M. Kleiner, L. Sylow, D. J. Fazakerley, J. R. Krycer, K. C. Thomas, A. J. Oxboll, A. B. Jordy, T. E. Jensen, G. Yang, P. Schjerling, B. Kiens, D. E. James, M. A. Ruegg, E. A. Richter, Acute mTOR inhibition induces insulin resistance and alters substrate utilization in vivo. *Mol. Metab.* **3**, 630–641 (2014).
- Z. Mao, W. Zhang, Role of mTOR in glucose and lipid metabolism. *Int. J. Mol. Sci.* **19**, 2043 (2018).
- M. J. Pereira, J. Palming, M. Rizell, M. Aureliano, E. Carvalho, M. K. Svensson, J. W. Eriksson, mTOR inhibition with rapamycin causes impaired insulin signalling and glucose uptake in human subcutaneous and omental adipocytes. *Mol. Cell. Endocrinol.* **355**, 96–105 (2012).
- F. Tremblay, A. Gagnon, A. Veilleux, A. Sorisky, A. Marette, Activation of the mammalian target of rapamycin pathway acutely inhibits insulin signaling to Akt and glucose transport in 3T3-L1 and human adipocytes. *Endocrinology* **146**, 1328–1337 (2005).
- K. Kim, L. Qiang, M. S. Hayden, D. P. Sparling, N. H. Purcell, U. B. Pajvani, mTORC1-independent Raptor prevents hepatic steatosis by stabilizing PHLPP2. *Nat. Commun.* **7**, 10255 (2016).
- H. Yang, X. Jiang, B. Li, H. J. Yang, M. Miller, A. Yang, A. Dhar, N. P. Pavletich, Mechanisms of mTORC1 activation by RHEB and inhibition by PRAS40. *Nature* **552**, 368–373 (2017).
- A. Scaiola, F. Mangia, S. Imseng, D. Boehringer, K. Berneiser, M. Shimobayashi, E. Stüttfeld, M. N. Hall, N. Ban, T. Maier, The 3.2-Å resolution structure of human mTORC2. *Sci. Adv.* **6**, eabc1251 (2020).
- L. S. Harrington, G. M. Findlay, A. Gray, T. Tolkacheva, S. Wigfield, H. Rebholz, J. Barnett, N. R. Leslie, S. Cheng, P. R. Shepherd, I. Gout, C. P. Downes, R. F. Lamb, The TSC1-2 tumor suppressor controls insulin-PI3K signaling via regulation of IRS proteins. *J. Cell Biol.* **166**, 213–223 (2004).
- O. J. Shah, Z. Wang, T. Hunter, Inappropriate activation of the TSC/Rheb/mTOR/S6K cassette induces IRS1/2 depletion, insulin resistance, and cell survival deficiencies. *Curr. Biol.* **14**, 1650–1656 (2004).
- Y. Yu, S. O. Yoon, G. Poulougiannis, Q. Yang, X. M. Ma, J. Villen, N. Kubica, G. R. Hoffman, L. C. Cantley, S. P. Gygi, J. Blenis, Phosphoproteomic analysis identifies Grb10 as an mTORC1 substrate that negatively regulates insulin signaling. *Science* **332**, 1322–1326 (2011).
- P. P. Hsu, S. A. Kang, J. Rameseder, Y. Zhang, K. A. Ottina, D. Lim, T. R. Peterson, Y. Choi, N. S. Gray, M. B. Yaffe, J. A. Marto, D. M. Sabatini, The mTOR-regulated phosphoproteome reveals a mechanism of mTORC1-mediated inhibition of growth factor signaling. *Science* **332**, 1317–1322 (2011).
- I. Bjedov, J. M. Toivonen, F. Kerr, C. Slack, J. Jacobson, A. Foley, L. Partridge, Mechanisms of life span extension by rapamycin in the fruit fly *Drosophila melanogaster*. *Cell Metab.* **11**, 35–46 (2010).
- S. C. Johnson, P. S. Rabinovitch, M. Kaeblerlein, mTOR is a key modulator of ageing and age-related disease. *Nature* **493**, 338–345 (2013).

42. J. Li, S. G. Kim, J. Blenis, Rapamycin: One drug, many effects. *Cell Metab.* **19**, 373–379 (2014).
43. O. Johnston, C. L. Rose, A. C. Webster, J. S. Gill, Sirolimus is associated with new-onset diabetes in kidney transplant recipients. *J. Am. Soc. Nephrol.* **19**, 1411–1418 (2008).
44. J. Xie, X. Wang, C. G. Proud, mTOR inhibitors in cancer therapy. *F1000Res.* **5**, F1000 (2016).
45. C. C. Thoreen, D. M. Sabatini, Rapamycin inhibits mTORC1, but not completely. *Autophagy* **5**, 725–726 (2009).
46. A. Y. Choo, S. O. Yoon, S. G. Kim, P. P. Roux, J. Blenis, Rapamycin differentially inhibits S6Ks and 4E-BP1 to mediate cell-type-specific repression of mRNA translation. *Proc. Natl. Acad. Sci. U.S.A.* **105**, 17414–17419 (2008).
47. A. D. Barlow, J. Xie, C. E. Moore, S. C. Campbell, J. A. Shaw, M. L. Nicholson, T. P. Herbert, Rapamycin toxicity in MIN6 cells and rat and human islets is mediated by the inhibition of mTOR complex 2 (mTORC2). *Diabetologia* **55**, 1355–1365 (2012).
48. D. W. Lamming, L. Ye, P. Katajisto, M. D. Goncalves, M. Saitoh, D. M. Stevens, J. G. Davis, A. B. Salmon, A. Richardson, R. S. Ahima, D. A. Guertin, D. M. Sabatini, J. A. Baur, Rapamycin-induced insulin resistance is mediated by mTORC2 loss and uncoupled from longevity. *Science* **335**, 1638–1643 (2012).
49. K. H. Schreiber, S. I. Arriola Apelo, D. Yu, J. A. Brinkman, M. C. Velarde, F. A. Syed, C. Y. Liao, E. L. Baar, K. A. Carbajal, D. S. Sherman, D. Ortiz, R. Brunauer, S. E. Yang, S. T. Zzannis, B. K. Kennedy, D. W. Lamming, A novel rapamycin analog is highly selective for mTORC1 in vivo. *Nat. Commun.* **10**, 3194 (2019).
50. S. J. Mahoney, S. Narayan, L. Molz, L. A. Berstler, S. A. Kang, G. P. Vlasuk, E. Saiah, A small molecule inhibitor of Rheb selectively targets mTORC1 signaling. *Nat. Commun.* **9**, 548 (2018).
51. S. A. Kang, D. J. O'Neill, A. W. Machl, C. J. Lumpkin, S. N. Galda, S. Sengupta, S. J. Mahoney, J. J. Howell, L. Molz, S. Hahm, G. P. Vlasuk, E. Saiah, Discovery of small-molecule selective mTORC1 inhibitors via direct inhibition of glucose transporters. *Cell Chem. Biol.* **26**, 1203–1213.e13 (2019).
52. M. D. Lacher, R. Pincheira, Z. Zhu, B. Camoretti-Mercado, M. Matli, R. S. Warren, A. F. Castro, Rheb activates AMPK and reduces p27Kip1 levels in Tsc2-null cells via mTORC1-independent mechanisms: Implications for cell proliferation and tumorigenesis. *Oncogene* **29**, 6543–6556 (2010).
53. Y. Ehinger, Z. Zhang, K. Phamluong, D. Soneja, K. M. Shokat, D. Ron, Brain-specific inhibition of mTORC1 by a dual drug strategy: A novel approach for the treatment of alcohol use disorder. *bioRxiv* 2020.10.12.336701 (2020).
54. N. Luong, C. R. Davies, R. J. Wessells, S. M. Graham, M. T. King, R. Veech, R. Bodmer, S. M. Oldham, Activated FOXO-mediated insulin resistance is blocked by reduction of TOR activity. *Cell Metab.* **4**, 133–142 (2006).
55. A. A. Teleman, Y. W. Chen, S. M. Cohen, 4E-BP functions as a metabolic brake used under stress conditions but not during normal growth. *Genes Dev.* **19**, 1844–1848 (2005).
56. A. J. Clippinger, T. G. Maguire, J. C. Alwine, The changing role of mTOR kinase in the maintenance of protein synthesis during human cytomegalovirus infection. *J. Virol.* **85**, 3930–3939 (2011).
57. N. Cybulski, V. Zinzalla, M. N. Hall, Inducible raptor and rictor knockout mouse embryonic fibroblasts. *Methods Mol. Biol.* **821**, 267–278 (2012).
58. I. Arganda-Carreras, V. Kaynig, C. Rueden, K. W. Eliceiri, J. Schindelin, A. Cardona, H. S. Seung, Trainable Weka Segmentation: A machine learning tool for microscopy pixel classification. *Bioinformatics* **33**, 2424–2426 (2017).
59. J. R. Krycer, L. Phan, A. J. Brown, A key regulator of cholesterol homeostasis, SREBP-2, can be targeted in prostate cancer cells with natural products. *Biochem. J.* **446**, 191–201 (2012).
60. J. R. Krycer, L. E. Quek, D. Francis, D. J. Fazakerley, S. D. Elkington, A. Diaz-Vegas, K. C. Cooke, F. C. Weiss, X. Duan, S. Kurdyukov, P. X. Zhou, U. K. Tambar, A. Hirayama, S. Ikeda, Y. Kamei, T. Soga, G. J. Cooney, D. E. James, Lactate production is a prioritized feature of adipocyte metabolism. *J. Biol. Chem.* **295**, 83–98 (2020).
61. C. Pfeifferberger, B. C. Lear, K. P. Keegan, R. Allada, Locomotor activity level monitoring using the *Drosophila* Activity Monitoring (DAM) System. *Cold Spring Harb Protoc* **2010**, pdb.prot5518 (2010).

**Acknowledgments:** We thank M. Hall for providing iRapKO and iRicKO MEF cells.

**Funding:** This work was supported by National Health and Medical Research Council (NHMRC) project grant (GNT1120201) and National Institutes of Health (NIH) grant (1R01CA221969). K.M.S. was supported by the Samuel Waxman Research Foundation. J.R.K. was supported by an Australian Diabetes Society Skip Martin Early-Career Fellowship. M.L. is a Cancer Institute NSW Future Research Leader Fellow. Z.Z. is a Damon Runyon Fellow supported by the Damon Runyon Cancer Research Foundation (DRG-2281-17). D.E.J. is an NHMRC Senior Principal Research Fellow. **Author contributions:** G.Y. designed the experiments, performed molecular biology and all cell experiments, analyzed the data, wrote the manuscript, and supervised the work. D.F. designed the experiments, performed *Drosophila* experiments, analyzed the data, and wrote the manuscript. J.R.K. performed measurement of lactate production and wrote the manuscript. M.L. performed size-exclusion chromatography. Z.Z., C.J.N., and K.M.S. synthesized RapaLink1. A.D.-V. analyzed the data of colony formation. D.E.J. designed experiments, wrote the manuscript, and supervised the work. **Competing interests:** K.M.S. is an inventor on patents (10,117,945 and 10,646,577) owned by UCSF covering RapaLink-1, which are licensed to Revolution Medicines. K.M.S. has consulting agreements for the following companies, which involve monetary and/or stock compensation: Revolution Medicines, Black Diamond Therapeutics, BridGene Biosciences, Denali Therapeutics, Dice Molecules, eFFECTOR Therapeutics, Erasca, Genentech/Roche, Janssen Pharmaceuticals, Kumquat Biosciences, Kura Oncology, Mitokinin, Type6 Therapeutics, Venthera, Wellspring Biosciences (Araxes Pharma), Turning Point, Ikena, Initial Therapeutics, and BioTheryX. The other authors declare that they have no competing interests. **Data and materials availability:** All data needed to evaluate the conclusions in the paper are present in the paper or the Supplementary Materials.

Submitted 26 July 2020

Resubmitted 28 January 2021

Accepted 2 September 2021

Published 21 September 2021

10.1126/scisignal.abe0161

**Citation:** G. Yang, D. Francis, J. R. Krycer, M. Larance, Z. Zhang, C. J. Novotny, A. Diaz-Vegas, K. M. Shokat, D. E. James, Dissecting the biology of mTORC1 beyond rapamycin. *Sci. Signal.* **14**, eabe0161 (2021).

## Dissecting the biology of mTORC1 beyond rapamycin

Guang Yang Deanne Francis James R. Krycer Mark Larance Ziyang Zhang Chris J. Novotny Alexis Diaz-Vegas Kevan M. Shokat David E. James

*Sci. Signal.*, 14 (701), eabe0161. • DOI: 10.1126/scisignal.abe0161

### A tale of two complexes

The kinase mTOR is a component of two multiprotein complexes, mTORC1 and mTORC2, which have distinct cellular functions. The compound rapamycin does not completely inhibit the kinase activity of mTORC1 and partially inhibits that of mTORC2 in certain cell types. Yang *et al.* used the rapamycin derivative RapaLink1 to differentiate between those functions mediated by mTORC1 and mTORC2. Because RapaLink1 had improved specificity for mTORC1 compared to rapamycin, the authors showed that cell proliferation and autophagy were regulated by mTORC1, whereas glycolysis was regulated by both complexes, and that starvation resistance in *Drosophila* was mediated by TORC1. These results demonstrate the utility of RapaLink1 in characterizing the cellular processes regulated by mTORC1 and mTORC2.

### View the article online

<https://www.science.org/doi/10.1126/scisignal.abe0161>

### Permissions

<https://www.science.org/help/reprints-and-permissions>

Use of this article is subject to the [Terms of service](#)

---

*Science Signaling* (ISSN ) is published by the American Association for the Advancement of Science, 1200 New York Avenue NW, Washington, DC 20005. The title *Science Signaling* is a registered trademark of AAAS.

Copyright © 2021 The Authors, some rights reserved; exclusive licensee American Association for the Advancement of Science. No claim to original U.S. Government Works